Eur. Phys. J. B **39**, 41–47 (2004)
DOI: 10.1140/epjb/e2004-00168-y

THE EUROPEAN PHYSICAL JOURNAL B

Constant pressure reactive molecular dynamics simulations of phase transitions under pressure: The graphite to diamond conversion revisited

F. Zipoli[1], M. Bernasconi[1,a], and R. Martoňák[2,b]

[1] Dipartimento di Scienza dei Materiali and Istituto Nazionale per la Fisica della Materia, Università degli Studi di Milano-Bicocca, Via Cozzi 53, 20125 Milano, Italy
[2] Computational Science, Department of Chemistry and Applied Biosciences, ETH Zurich, USI Campus, Via Giuseppe Buffi 13, 6900 Lugano, Switzerland

Received 11 February 2004
Published online 18 June 2004 –

Abstract. We have introduced a new technique for constant-pressure molecular dynamics by combining the idea behind the Parrinello-Rahman scheme and the method by Iannuzzi, Laio and Parrinello [Phys. Rev. Lett. **90**, 238302 (2003)], recently devised to deal with rare events. The new scheme is suitably devised to describe solid-solid phase transitions for which the primary order parameter is not the cell shape, but some internal structural coordinate. The method has been demonstrated by simulating the conversion of graphite into diamond at high pressure within a tight-binding model.

PACS. 61.50.Ks Crystallographic aspects of phase transformations; pressure effects

1 Introduction

The study of phase transitions under pressure is a very active area of research [1]. The experimental investigation of matter at extreme conditions of pressure and temperature is often very demanding and can benefit from the aid of theoretical simulations suitable to provide possible candidates for the structures stable at high pressure and temperature. In this respect, the predictive power of molecular dynamics simulations has been greatly improved with the introduction of the constant-pressure Parrinello-Rahman (PR) technique [2] and its implementation in the ab-initio Car-Parrinello method [3]. However, in PR simulations a first-order phase transition does not proceed via nucleation and growth as expected in the real system, instead it often takes place as a collective transformation occurring across the whole simulation cell. As a consequence the system has to cross a significant free energy barrier to transform from one structure to another and the activation barrier must often be reduced by overpressurization in order to observe the transition within the accessible simulation time. Under these conditions intermediate phases may be skipped which reduces the predictive power of the method.

An important step to overcome these limitations has been put forward by Martoňák, Laio and Parrinello (MLP) [4] who developed a new method to study pressure-induced structural transformation by adapting an approach previously devised by Laio and Parrinello [5] to observe rare events within molecular dynamics simulations. As in the PR scheme, MLP used the edges of the simulation cell $\mathbf{h} = (\vec{a}, \vec{b}, \vec{c})$ as dynamical variables. However, in place of the second order equation of motion of the PR scheme, in the MLP method the cell edges evolve according to a first-order steepest-descent-like dynamics (metadynamics) under the effect of the imbalance between the internal stress and the external applied pressure and of an external history-dependent potential which drives the system away from the local minimum towards a new crystal structure. The history-dependent potential is given by the sum of Gaussian functions centered at every point already visited by the cell edges along the metadynamics trajectory and acts as to discourage the system from visiting them again. This Gaussian potential, which fills the free energy basins in the configuration space spanned by the cell edges, can also be introduced in a continuous dynamics which would amount to simply add the Gaussian history-dependent potential of reference [4] to the Parrinello-Rahman Lagrangian. The advantages of the MPL method have been demonstrated by reproducing the phase transition of silicon at the theoretical transition pressure whereas the PR dynamics requires a pressure three times as large.

[a] e-mail: marco.bernasconi@mater.unimib.it
[b] *Permanent address*: Department of Physics, Faculty of Electrical Engineering and Information Technology, Slovak University of Technology, Ilkovičova 3, 812 19 Bratislava, Slovakia.

However, the MPL scheme still suffers from some limitations in common with the original PR method. For instance the MPL is less effective for the study of phase transitions for which the primary order parameter is an internal coordinate instead of the cell edges. This is the case for phase transformations under pressure described in terms of solid state chemical reactions such as the 2D [6] and 3D [7] polymerizations of C_{60} or the topochemical solid-state polymerizations of alkenes, alkynes and aromatic hydrocarbons [8,9]. For instance, in the 2D polymerization of C_{60} the activation barrier for the [2+2] cycloaddition reaction is overcome by a suitable deformation of the fullerenic cage which is not induced by simply decreasing the intercage distances down to the density of the 2D polymer [10]. In the perspective to address the study of phase transformations in this class of materials, we here present an extension to constant-pressure simulations of the scheme recently devised by Iannuzzi, Laio and Parrinello (ILP) [11] to deal with the molecular dynamics simulation of complex chemical reactions with large activation barriers. The ILP scheme can be dubbed *reactive* molecular dynamics since suitably defined reaction coordinates are introduced as dynamical variables. By combining the ideas behind the PR and ILP methods we introduce a constant-pressure *reactive* molecular dynamics scheme and demonstrate its validity by simulating the conversion of carbon from graphite to diamond under pressure. This latter transformation as well can be seen as driven by an internal order parameter: the corrugation of the graphitic planes leading to the change of hybridization of carbon from sp^2 to sp^3. Graphite thus represents a simpler system to show the capabilities of the new scheme and its advantages with respect to the PR method. The graphite to diamond conversion has been already reproduced in the ab-initio PR molecular dynamics simulations of reference [12] although at a pressure (90 GPa) four times larger than the experimental estimate (15 GPa, [13]) due to the aforementioned limitations of the PR method. In the present work graphite is described by the tight-binding (TB) potential of reference [14] supplemented by an empirical two-body van der Waals (vdW) interaction, necessary to describe the interplanar distance in graphite. Within the new simulation scheme graphite transforms to diamond at the theoretical transition density at room temperature whereas within a PR simulation no transformation is observed for this model (TB) of graphite even if temperature is increased up to 1000 K and pressure up to four times the theoretical transition pressure. The method is described in Section 2 and its application to graphite is presented in Section 3 below.

2 Methodology

2.1 General scheme

By combining the ideas behind the PR and ILP methods we introduce a constant-pressure *reactive* molecular dynamics described by a Lagrangian of the form

$$\begin{aligned}\mathcal{L} =& \frac{1}{2}\sum_{i=1}^{N} m_i(\dot{\mathbf{s}}_i^t \mathbf{h}^t \mathbf{h} \dot{\mathbf{s}}_i) - E(\{\mathbf{s}_i\},\mathbf{h}) + \frac{1}{2} W_c Tr \dot{\mathbf{h}}^t \dot{\mathbf{h}} - p\Omega \\ &+ \sum_\alpha \frac{1}{2} M_\alpha \dot{\eta}_\alpha^2 - \sum_\alpha \frac{1}{2} k_\alpha \big(\eta_\alpha(\{\mathbf{s}_i\},\mathbf{h}) - \eta_\alpha\big)^2 \\ &- V(t,\{\eta_\alpha\}), \end{aligned} \tag{1}$$

where the first line is the PR Lagrangian [2] and the second line is the ILP Lagrangian [11]. $\mathbf{s}_i$ are scaled ionic coordinates, Ω is the cell volume, p the external pressure and η_α are collective variables as in the ILP scheme [11] with a fictitious kinetic energy and mass (M_α). A harmonic potential restrains the values of the collective coordinates $\eta_\alpha(\{\mathbf{s}_i\},\mathbf{h})$ close to the corresponding dynamical collective variables η_α. The values of M_α and k_α are chosen in such a way as to separate adiabatically the motion of the collective variables from the ionic one as discussed in reference [11]. The collective coordinates $\eta_\alpha(\{\mathbf{s}_i\},\mathbf{h})$ are functions of the scaled ionic coordinates and of the cell edges and should be able to discriminate between the initial and final phases. $E(\{\mathbf{s}_i\},\mathbf{h})$ is the total internal energy while $V(\{\eta_\alpha\},t)$ is the history-dependent potential acting on the collective variables and given by

$$V(t,\{\eta_\alpha\}) = \sum_{t'<t} W \prod_\alpha e^{-\frac{|\eta_\alpha - \eta_\alpha^{t'}|^2}{2\sigma_\alpha^2}}, \tag{2}$$

where W and σ_α are suitable chosen parameters as described in reference [5]. The equations of motion corresponding to the Lagrangian (1) are

$$\begin{aligned} m_i \ddot{\mathbf{s}}_i =& -\frac{\partial E(\{\mathbf{s}_i\},\mathbf{h})}{\partial \mathbf{s}_i}\mathbf{G}^{-1} - m_i \mathbf{G}^{-1}\dot{\mathbf{G}}\dot{\mathbf{s}}_i \\ &+ k_\alpha(\eta_\alpha(\{\mathbf{s}_i\},\mathbf{h}) - \eta_\alpha)\frac{\partial \eta_\alpha(\{\mathbf{s}_i\},\mathbf{h})}{\partial \mathbf{s}_i}\mathbf{G}^{-1}, \\ W_c \ddot{\mathbf{h}} =& (\pi - p\mathbb{I})\Omega(\mathbf{h}^t)^{-1}, \\ M_\alpha \ddot{\eta}_\alpha =& -k_\alpha(\eta_\alpha(\{\mathbf{s}_i\},\mathbf{h}) - \eta_\alpha) + \frac{\partial V(t,\{\eta_\alpha\})}{\partial \eta_\alpha} \end{aligned} \tag{3}$$

where $\mathbf{G} = \mathbf{h}^t\mathbf{h}$ and

$$\begin{aligned}\pi = \frac{1}{\Omega}\Bigg(&\sum_{i=1}^{N}(m_i \dot{\mathbf{s}}_i \mathbf{h}^t \mathbf{h} \dot{\mathbf{s}}_i) - \frac{\partial E(\{\mathbf{s}_i\},\mathbf{h})}{\partial \mathbf{h}}\mathbf{h}^t \\ &- \sum_\alpha k_\alpha(\eta_\alpha(\{\mathbf{s}_i\},\mathbf{h}) - \eta_\alpha)\frac{\partial \eta_\alpha(\{\mathbf{s}_i\},\mathbf{h})}{\partial \mathbf{h}}\mathbf{h}^t\Bigg) \end{aligned} \tag{4}$$

is the internal stress including a contribution from the harmonic restrain potential in (1).

2.2 Computational details for the simulation of graphite

To demonstrate the validity of the new scheme described above we have simulated the conversion of carbon from

graphite to diamond under pressure. This transformation can be seen as driven by an internal order parameter such as the corrugation of the graphitic planes which leads to the change of hybridization of carbon from sp^2 to sp^3. As a measure of the hybridization type of the carbon atoms, we have defined as collective variable the coordination number of the atoms of a single graphitic plane in the simulation cell with respect to the atoms of the two neighboring planes, i.e.

$$\eta = \sum_{i \in plane} \sum_{j \notin plane} c_{ij}, \tag{5}$$

with

$$c_{ij} = \frac{1 - (\frac{r_{ij}}{d})^6}{1 - (\frac{r_{ij}}{d})^{12}}, \tag{6}$$

where r_{ij} is the distance between atoms i and j and $d = 2.2$ Å. The energy term $E(\{\mathbf{s}_i\}, \mathbf{h})$ in equation (1) is given by the tight-binding potential of reference [14] supplemented by an empirical two-body van der Waals interaction, necessary to describe the interplanar distance in graphite. Details on the van der Waals interatomic potential are given in the Appendix. Calculations are performed with a supercell containing 128 atoms initially arranged in the graphite structure with four graphitic planes per cell in the ABAB (hexagonal) stacking [12]. Only the supercell Γ point has been included in the Brillouin Zone integration. The calculated equation of state (EOS) of graphite at zero temperature has been fitted by a Murnaghan function [15] close to the equilibrium volume (inset of Fig. 1a) which corresponds to the equilibrium lattice parameters $a = 2.46$ Å (exp. 2.46 Å [16]) and $c = 6.82$ Å (exp. 6.70 Å [16]) and bulk modulus $B = 28$ GPa (exp. 35.8 GPa [17]) in good agreement with the experimental values. The c/a ratio in graphite as a function of volume is reported in Figure 1b; the change in slope is associated to a change in the stacking of the graphitic plane from the hexagonal (ABAB) stacking at low pressure to the orthorombic stacking at high pressure (cf. Ref. [12]). The equilibrium lattice parameter and bulk modulus of diamond calculated with a commensurate 128-atoms supercell are $a = 3.552$ Å (exp. 3.566 Å [16]) and $B = 473$ GPa (exp. 442 GPa [18]) [19]. The calculated EOS of graphite and diamond are reported in Figure 1a. The compressibility of graphite is well reproduced close to the equilibrium volume, but it is drastically overestimated at lower volumes. As a consequence the theoretical transition pressure to diamond is as high as 129 GPa (exp. 15 GPa [13]) and the volume jump at the transition pressure is very small, the volume being 4.70 Å^3/atom for graphite and 4.60 Å^3/atom for diamond (cf. the ab-initio EOS of graphite and diamond of Ref. [12]). These results highlight the inadequacy of the TB+vdW model to describe correctly graphite at high pressure. Nevertheless this model graphite represents a good testing case for the new simulation scheme. In fact, the small volume jump at the theoretical transition pressure prevents the reduction of the activation barrier by overpressurization and consequently the transition to diamond does not take place in a

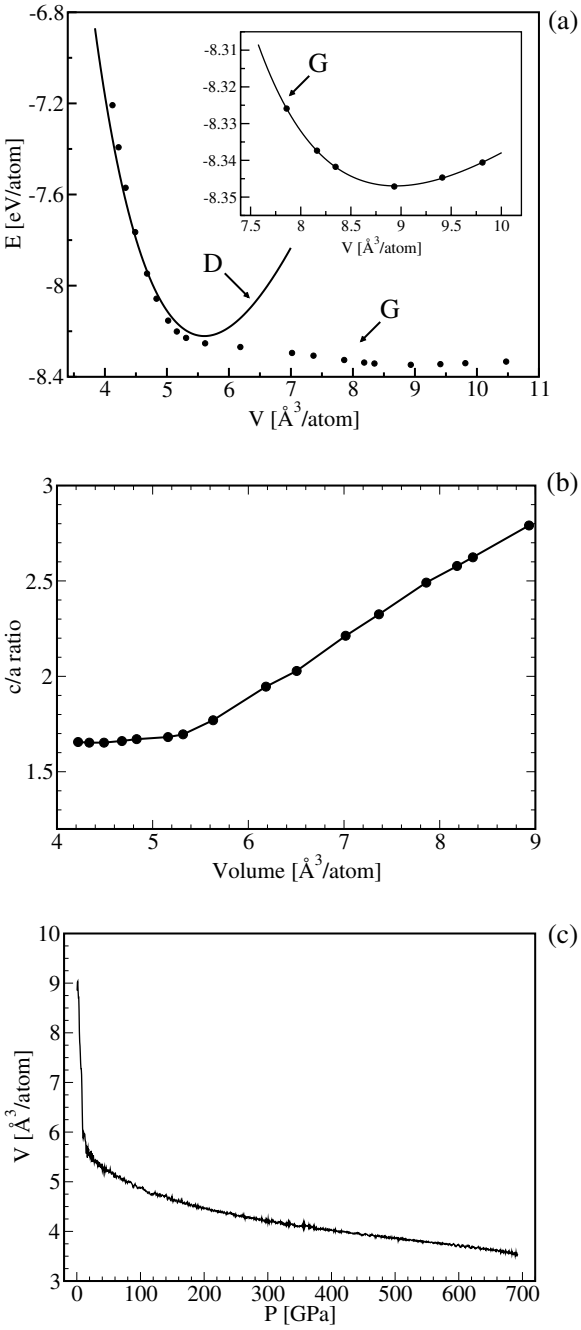

Fig. 1. (a) Equation of state of state of graphite (G, dots) and diamond (D, continuous line) obtained with the tight-binding model (see text). Inset: equation of state of graphite close to the equilibrium volume. (b) Ratio c/a in graphite as a function of volume. (c) Volume versus pressure in a Parrinello-Rahman simulation of graphite at 1000 K (see text).

PR simulation (70 ps long) even by increasing the pressure up to 700 GPa and temperature up to 1000 K. The pressure versus volume curve in the PR simulation is reported in Figure 1c. Conversely, we will show in Section 3 that within the new simulation scheme, the transformation to diamond occurs very close to the theoretical transition density. In the simulations reported in the next section,

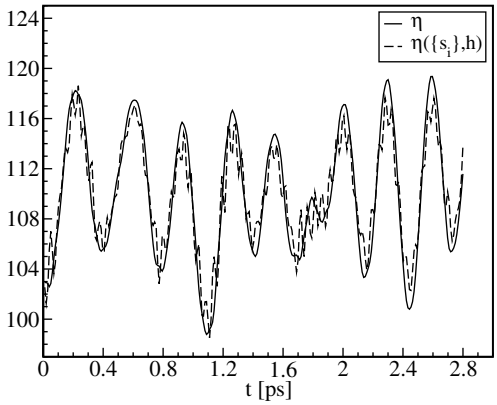

Fig. 2. Free evolution in time of the collective coordinate $\eta(\{\mathbf{s}_i\}, \mathbf{h})$ (continuous line, Eq. (5)) and of the corresponding dynamical collective variable η (dashed line) in a constant-pressure simulation of graphite at 15 GPa and 300 K. The history-dependent Gaussian potential is not added.

the fictitious mass and spring constant of the collective variable (Eq. (5)) are $M = 0.24$ amu Å^2 and $k = 0.04$ eV. The evolution in time of the dynamical collective variable η and of the corresponding collective coordinate $\eta(\{\mathbf{s}_i\}, \mathbf{h})$ is shown in Figure 2 for a free (without Gaussian potential, Eq. (2)) constant-pressure simulation at 15 GPa and 300 K. The ionic temperature is controlled by velocity rescaling with a tolerance of 10% on the target temperature. As is clear from Figure 2, the values chosen for M and k ensure a good restrain of the collective coordinate to the corresponding dynamical variable. The height and width of the Gaussian functions of the history-dependent potential of equation (2) are $W = 3$ eV and $\sigma = 10.0$ according to the general prescriptions given in references [5,11]. A Gaussian is added whenever η changes by 15 units or after 80 fs of simulation. We have also repeated the simulations at higher temperature (1000 K) and with different parameters of the Gaussian functions ($W = 7$ eV and $\sigma = 15.0$, and $W = 4$ eV and $\sigma = 10.0$) with results similar to those reported in next section. In all simulations the fictitious mass of the cell is $W_C = 128$ amu [20] and the integration time step is 0.51 fs. A predictor-corrector integrator of order five is used.

3 Results

We have performed a constant-pressure simulation of graphite according to equation (3) at 15 GPa and 300 K. The Gaussian potential acting on the collective variable of equation (5) is added as described in Section 2. The simulation cell is initially equilibrated at 15 GPa and 300 K within standard PR dynamics. The evolution in time of the edges, angles and volume of the simulation cell and of the collective coordinate $\eta(\{\mathbf{s}_i\}, \mathbf{h})$ is shown in Figure 3. During the simulation run, 28 ps long, we have observed several (of the order of 15) forward and backward transitions between graphite and diamond. Since there is a small volume jump at the transition point, the transformation

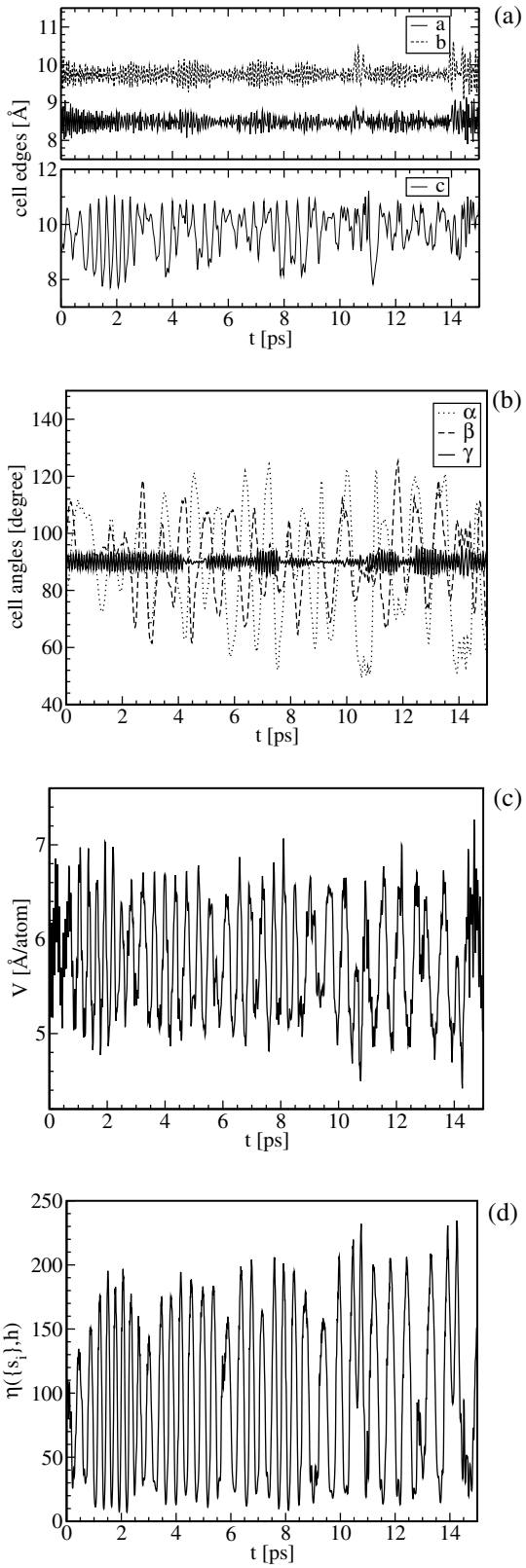

Fig. 3. Evolution in time of the (a) cell edges, (b) cell angles and (c) cell volume in a constant-pressure simulation at 15 GPa and 300 K within the new simulation scheme. The cell edges a and b lye on the graphitic planes while c is initially parallel to the [0001] direction of graphite. (d) Evolution in time of the collective coordinate $\eta(\{\mathbf{s}_i\}, \mathbf{h})$ (see text).

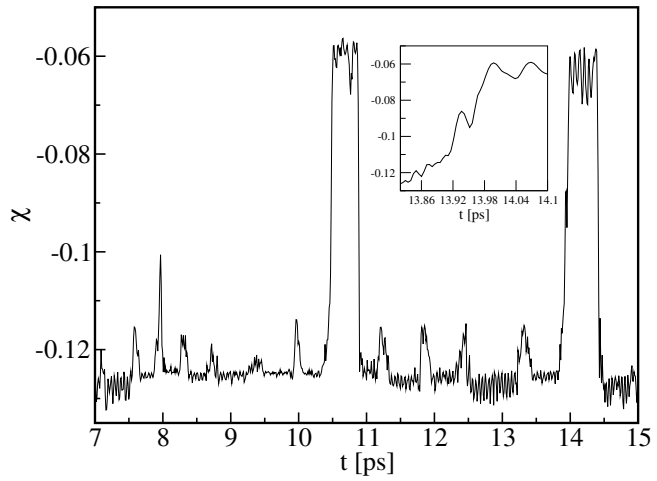

Fig. 4. Evolution in time of the indicator χ (see Eq. (7) in the text) which discriminates between the structures of graphite and diamond. Only the first part of the simulation is reported for sake of clarity. The inset reports a magnification of the time interval around 14 ps where the second transition to diamond occurs. Along the whole run 28 ps long, we have seen 15 jumps of χ similar to those reported in the figure which equally correspond to oscillations between graphite and diamond.

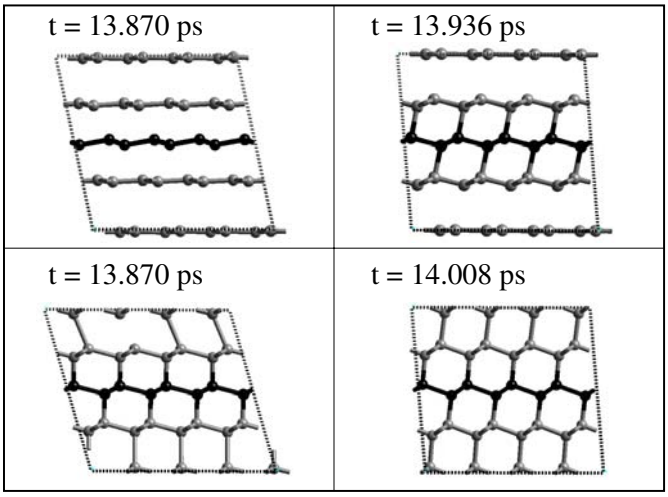

Fig. 5. The transformation path from graphite to diamond occurring at 14.0 ps from selected snapshots of the atomic trajectory (cf. Figs. 4 and 3). The simulation cell and the time scale are also reported. The atoms depicted by dark spheres correspond to the plane to which the collective variable of equation (5) refers to.

in not easily recognizable by inspection on the evolution of the cell parameters. The collective coordinate of equation 5 as well, although suitable to induce the transformation, it is not able to clearly discriminate between the two phases at very high pressure. We has thus introduced the indicator χ which provides a sharper distinction between the hybridization states of carbon atoms as

$$\chi = \frac{1}{N}\sum_i \frac{1}{n_i}\sum_{j>k} n_{ij} n_{ik} \cos^3\theta_{ijk} \qquad (7)$$

where

$$n_i = \sum_{j\neq i} n_{ij},$$
$$n_{ij} = \frac{1}{1+e^{(r_{ij}-d)/\Delta}}, \qquad (8)$$

with $d = 1.8$ Å and $\Delta = 0.05$ Å. The index i runs over all the N atoms of the simulation cell and n_i is the coordination number of atom ith. The index k and j run over atoms neighboring to atom ith and θ_{ijk} is the angle subtended by the tern ijk whose contribution to χ is weighted by the product of the partial coordination number n_{ik} and n_{ij}. The cosine function in (7) is able to discriminate between the hybridization sp^2 and sp^3. In fact the indicator χ is –0.125 for graphite and –0.06 for diamond at 15 GPa and 300 K. The time evolution of χ is reported in Figure 4 only for the first part of the run for sake of clarity. Two transitions from graphite to diamond are clearly identified at 10.5 ps and at 14.0 ps. Similarly, other twelve transformations can be identified in the other 12 ps of simulation. As discussed in reference [5], the Gaussian potential fills first the free-energy basin corresponding to graphite and, once the system is driven to the new phase, the basin corresponding to the final structure is then progressively filled. Once both basins are filled, the system is able to oscillate from one structure to the other. The transformations at 10.5 and 14.0 ps take place by a nucleation of the diamond structure on the three planes involved in the definition of the collective coordinate (Eq. (5)) and then propagates rapidly inducing a change in the cell shape (a jump to lower values of the c axis and of the α angle, cf. Figs. 4 and 3). The nucleus survives longer in the transformation at 14.0 ps showing up as a smaller peak in the rise of χ (inset of Fig. 4). The transformation at 10.5 ps (14.0 ps) starts at a volume of 4.45 Å^3/atom (4.70 Å^3/atom) very close to the theoretical transition volume of 4.70 Å^3/atom obtained from the EOS of graphite and diamond. The nucleus of diamond forms by aligning in the ABC stacking the three planes involved in the definition of the collective coordinate (Eq. (5)). Then to complete the transformation, the cell changes shape by aligning in the ABC stacking the other planes as well which finally produces a diamond structure with the [111] direction aligned to the original [0001] axis of graphite (cf. Refs. [12]). A snapshot of the atomic structure during the phase transition at 14.0 ps is reported in Figure 5. This transformation path is different from the mechanism identified in the ab-initio PR simulation of reference [12] which involves the formation of an intermediate orthorombic phase, although the orthorombic is the stable structure at high pressure also for our EOS of graphite (cf. Figs. 1a and 1b). As in the ab-initio PR simulation of reference [12], we have observed a fast sliding of

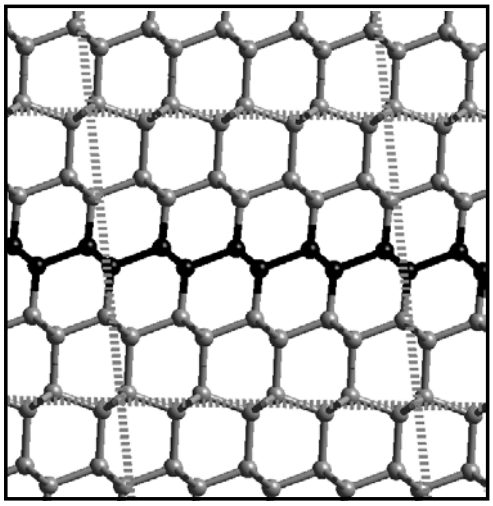

Fig. 6. The mixed phase of cubic and hexagonal diamond in one of the phase transition observed. The edges of the unit cells are also shown.

the graphitic planes which assume many different stacking geometries including the orthorombic phase. The discrepancy with the ab-initio result on the transformation path might be either due to the formation of a nucleus in the present simulation as opposed to the collective transformation of reference [12], or it might most probably originate from the inadequacy of the TB model in describing the interplanar interaction in graphite at high pressure. In fact, the underestimation of the interplanar repulsion would also imply a smaller energy difference between the hexagonal and orthorombic phases. Nevertheless, the issue here is that the new technique has been demonstrated to correctly reproduce the structure of the phase stable at high pressure by providing a spontaneous transformation at the theoretical equilibrium volume whereas the PR method fails [23]. Moreover, in agreement with the ab-initio PR simulation of reference [12], some of the structures observed during the oscillations from graphite to diamond are a mixture of cubic and hexagonal diamond (see Fig. 6). These results demonstrate the effectiveness of the constant-pressure scheme presented in Section 2. However, for the particular application presented here, we must say that the MPL scheme as well is able to reproduce the phase transition at the theoretical equilibrium density. In fact, a transition from graphite to diamond at the volume of 4.84 Å^3 has also been observed in a PR simulation supplemented by the history-dependent Gaussian potential acting on the length of the c-axis only. Nevertheless, the results presented for graphite would encourage the application of our new scheme to other systems where its advantages with respect to the PR and MLP methods would show up more clearly. This would be the case of the 3D polymerization of C_{60} for which both the PR and MLP methods have already been demonstrated to fail in reproducing the phase transition from the 2D polymer to the ordered 3D polymeric structure observed experimentally.

4 Conclusion

In summary, we have introduced a new method for the simulation of solid-solid phase transitions by constant-pressure molecular dynamics. By combining the idea behind the Parrinello-Rahman scheme and the method by Iannuzzi, Laio and Parrinello [11] dealing with rare events, we have devised a new technique suitable to describe solid-solid phase transitions for which the primary order parameter is not the cell shape, but some internal structural coordinate. The applicability of the method has been demonstrated by simulating the conversion of graphite into diamond at high pressure within a tight-binding model. The transition occurs spontaneously at the theoretical transition density whereas it does not take place in a Parrinello-Rahman simulation (within the tight-binding model) even by overpressurizing the system up to five times the theoretical transition pressure.

This work is partially supported by MURST through project PRIN01-2001021133. We gratefully thank M. Iannuzzi, A. Laio and M. Parrinello for discussion and for sharing with us their insight on the new methods they have developed.

Appendix

We have supplemented the TB model of reference [14] with a two-body potential which includes the van der Waals (vdW) interaction, necessary to reproduce the interplanar distance of graphite. We have used the same vdW potential we previously used to simulate C_{60} fullerite in reference [21]. The additional two-body interaction is given by a Lennard-Jones potential $V_{LJ} = 4\epsilon((\sigma/r)^{12} - (\sigma/r)^6)$ with $\epsilon = 2.84385$ meV and $\sigma = 3.469$ Å [22]. This potential is active only at interatomic distances larger than the cutoff of the TB potential of reference [14] ($r_{cut} = 2.6$ Å) as $V_{vdW} = V_o$ for $r < r_{cut}$, $V_{vdW} = V_o + a(r - r_{cut})^2 + b(r - r_{cut})^3$ for $r_{cut} < r < r_{cut} + \delta_1$ and $V_{vdW} = V_{LJ}$ for $r > r_{cut} + \delta_1$. The parameters a, b and V_o are obtained by imposing the continuity of the function and its first derivative at the two boundaries r_{cut} and $r_{cut} + \delta_1$. The free parameter δ_1 has been fitted in reference [21] in order to reproduce the lattice parameter of fullerite. This potential is sufficiently transferable to reproduce the interplanar distance and compressibility of graphite at the equilibrium volume as described in Section 2.

References

1. *High Pressure Phenomena*, edited by R.J. Hemley, G.L. Chiarotti, M. Bernasconi, L. Ulivi, (Editrice Compositori, Bologna, 2002); *Proceeding of the CXLVII course of the school Enrico Fermi*, Varenna 2001
2. M. Parrinello, A. Rahman, Phys. Rev. Lett. **45**, 1196 (1980)

3. P. Focher, G.L. Chiarotti, M. Bernasconi, E. Tosatti, M. Parrinello, Europhys. Lett. **26**, 345 (1994)
4. R. Martoňák, A. Laio, M. Parrinello, Phys. Rev. Lett. **90**, 75503 (2003)
5. A. Laio, M. Parrinello, Proc. Nat. Acad. Sci. **99**, 12562 (2002)
6. Y. Iwasa et al., Science **264**, 1570 (1994)
7. L. Marques et al., Science **283**, 1720 (1999)
8. M. Bernasconi, G.L. Chiarotti, P. Focher, M. Parrinello, E. Tosatti Phys. Rev. Lett. **78**, 2008 (1997)
9. V. Schettino, R. Bini, Phys. Chem. Chem. Phys. **5**, 1951 (2003)
10. T. Ozaki, Y. Iwasa, T. Mitani, Chem. Phys. Lett. **285**, 289 (1998)
11. M. Iannuzzi, A. Laio, M. Parrinello, Phys. Rev. Lett. **90**, 238302 (2003)
12. S. Scandolo, M. Bernasconi, G.L. Chiarotti, P. Focher, E. Tosatti, Phys. Rev. Lett. **74**, 4015 (1995)
13. F.P. Bundy, J.S. Kasper, J. Chem. Phys. **46**, 3437 (1967)
14. C. Xu, C. Wang, C. Chan, K.-H. Ho, J. Phys.: Condens. Matter **4**, 6047 (1992)
15. F.D. Murnaghan, Proc. Nat. Acad. Sci. **30**, 244 (1944)
16. *CRC Handbook of Chemistry and Physics*, 78th edn. (CRC Press, Boca Raton 1997), pp. 12–19
17. O.L. Blakslee, et al., J. Appl. Phys. **41**, 3373 (1970)
18. H.J. McSkimin, W.L. Bond, Phys. Rev. **105**, 116 (1957)
19. The equilibrium total energy of graphite is 0.126 eV/atom lower than that of diamond while the corresponding experimental value is 0.02 eV/atom ([16]). This misfit can be also partially due to insufficient accuracy in the Brillouin Zone integration
20. M. Parrinello, in Molecular Dynamics Simulation of Statitical Mechanical Systems, *Proceeding of the course XCVII of the International School of Physics "Enrico Fermi"* (North-Holland Physics Publishing, Amsterdam, 1986)
21. A. Cavalleri, K. Sokolowski-Tinten, D. von der Linde, I. Spagnolatti, M. Bernasconi, G. Benedek, A. Podestà, P. Milani, Europhys. Lett. **57**, 281 (2002)
22. L.A. Girifalco, J. Chem. Phys. **95**, 5370 (1992); L.A. Girifalco, J. Chem. Phys. **96**, 858 (1992)
23. We here recall once again that the PR scheme fails for our particular model of graphite described by the TB+vdW interactions, while in the ab-initio PR simulation of reference [12] the transition to diamond does occur although at a pressure four times larger than the equilibrium pressure